

1 Double-layered Water Cherenkov Detector for SWGO

2 **Samridha Kunwar^{a,*} on behalf of the SWGO Collaboration**

3 (a complete list of authors can be found at the end of the proceedings)

4 ^aMax-Planck-Institut für Kernphysik (MPIK), Saupfercheckweg 1, 69117 Heidelberg, Germany

5 E-mail: samridha.kunwar@mpi-hd.mpg.de

6 The Southern Wide-field Gamma-ray Observatory (SWGO) will use the well-established and cost-effective technique of detecting Cherenkov light produced in water-filled detection units for TeV gamma-ray astronomy. Leveraging detector material reflectivity together with an optimised aspect ratio is an option to improve the performance of an array of such detector units. The double-layered Water Cherenkov Detector units comprise chambers with single photosensors in each. A reflective upper compartment enhances sensitivity to impinging secondary particles. A shallow lower compartment enables muon tagging and consequently improves the gamma hadron separation power of the observatory. Here we present detailed studies on the double-layered unit design.

37th International Cosmic Ray Conference (ICRC 2021)
July 12th – 23rd, 2021
Online – Berlin, Germany

*Presenter

1. Introduction

The induced electromagnetic cascade produced by air showers are well suited to be observed by ground-level particle detectors providing intrinsically wide field-of-view and $\sim 100\%$ duty cycle. HAWC (High-Altitude Water Cherenkov) [1] on the flanks of the Sierra Negra in Mexico, and LHAASO (Large High Altitude Air Shower Observatory) [2] in the eastern Tibetan plateau are the two main instruments currently under operation that comprise an array of Water Cherenkov Detector (WCD) units. The detection of γ -rays higher than 0.1 PeV have already been reported by LHAASO [3] and instrumenting the Southern Hemisphere will provide unprecedented opportunities to probe the galactic plane and the southern hemisphere further [4].

Furthermore, instrumenting at a High altitude (> 4.4 km) with a high fill factor ($> 80\%$) will allow SWGO to be complementary in the same energy range as Imaging Atmospheric Cherenkov Telescopes (IACTs). This is extended to an outer array with a fill factor of 8% as in Fig. 1 that aims to improve sensitivity at higher energies.

SWGO (for an overview on status and prospects, see [5]) is investigating several detector technologies such as units with multiple photo-sensors [6] and an option to deploy detector units in a lake [7]. Muon identification with a separate detector element is a reasonable means of hadronic background rejection (see, e.g. [8]) for γ -ray astronomy. Here we develop the concept of a double-layered WCD design; as a potential detector unit for SWGO, comprising two isolated chambers where the lower chamber in conjunction with the upper chamber enables an effective method for gamma/hadron separation. The detector unit with optimised aspect ratio and material reflectivity will also have improved particle detection efficiency and angular resolution.

The simulations in this work use GEANT4 [9] within a simulation framework adapted from the HAWC collaboration. Air Shower simulations use the CORSIKA 7.7400 simulation package [10] where we select the hadronic interaction model QGSJet-II.04 [11] for energies above 80 GeV. UrQMD 1.3.1 [12, 13] treats the low energy hadronic interactions and for electromagnetic processes, we use the EGS4 electromagnetic model [14].

2. Unit Design

The double-layered design comprises two chambers that are isolated from each other, as shown in Fig. 2. The upper chamber is a light-tight chamber with a reflective lining and a centrally located 8" Photo-Multiplier Tube (PMT) facing upwards. The PMT orientation ensures that the prompt

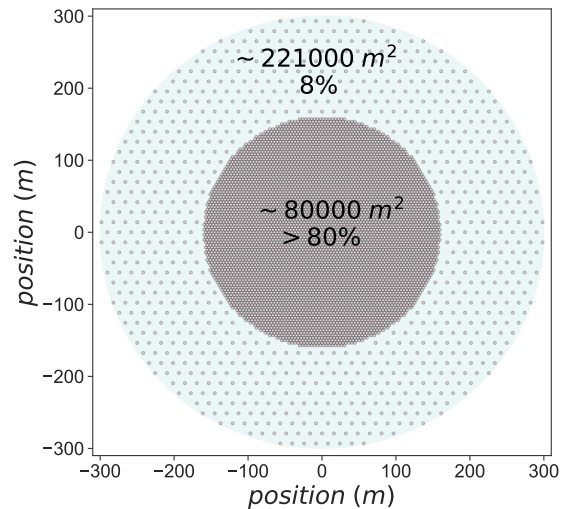


Figure 1: Sketch of the simulated array layout of cylindrical double-layered WCDs with a dense inner array ($> 80\%$) and sparser outer array ($\sim 8\%$).

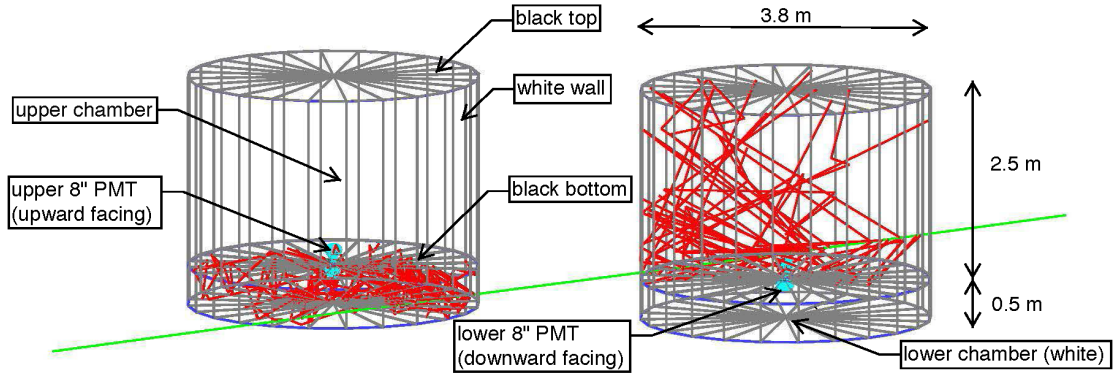


Figure 2: Cylindrical Double Layered WCD designs comprising an upper chamber ($\pi \times 1.91^2 \times 2.5 \text{ m}^3$) with white walls and black bases (top and bottom) and an entirely white lower chamber ($\pi \times 1.91^2 \times 0.5 \text{ m}^3$). The upper chamber comprises an 8" PMT facing upwards, and the lower chamber comprises an 8" PMT facing downwards. A Muon (green) passes through both units and produces photons (red). The number of photons has been limited here for illustration purposes.

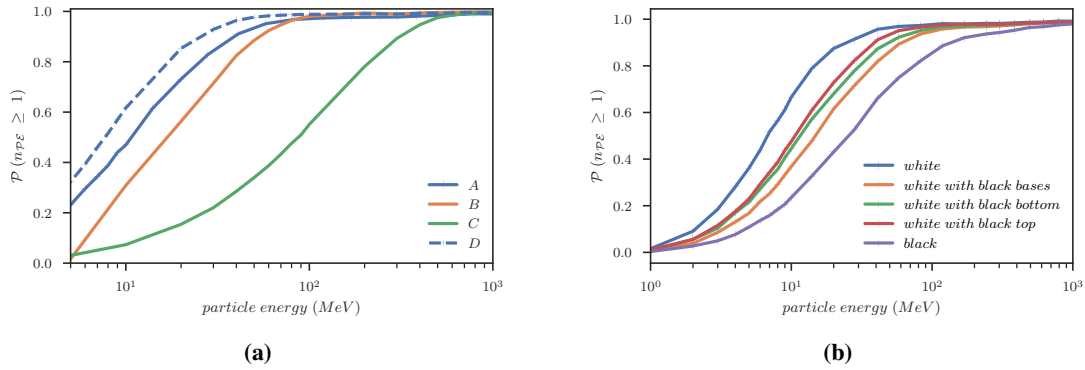


Figure 3: (a) Injection of vertical 5 MeV to 1 GeV γ -rays across the top surface of different WCD designs. Here we show a comparison between the upper chamber of a [A] white cylindrical double-layered WCD unit ($\pi \times 1.91^2 \times 2.5 \text{ m}^3$) with a black top and an 8" PMT, a [B] HAWC - like design ($\pi \times 3.65^2 \times 4 \text{ m}^3$) with black walls, a central 10" PMT and 3x8" PMTs, a [C] LHAASO - like black unit ($5 \times 5 \times 4.5 \text{ m}^3$) with an open top and an 8" PMT and a [D] white cylindrical double-layered WCD unit ($\pi \times 1.71^2 \times 3 \text{ m}^3$) with a black top and an 8" PMT. (b) Response to injection of vertical 1 MeV to 1 GeV γ -rays across the top of the upper chamber of double-layered WCD unit ($\pi \times 1.91^2 \times 2.5 \text{ m}^3$) with vertical 1 MeV to 1 GeV γ -rays with different materials.

47 light is detected first. The lower chamber is a similar light-tight chamber but, to ensure we collect
 48 all the energy deposited in the chamber for muon identification, it is composed of highly reflective
 49 material and a centrally located 8" PMT facing downwards.

50 3. Particle Detection Efficiency and Energy Resolution

51 The particle detection efficiency of the DLWCD is optimised by leveraging the aspect ratio
 52 and the material (reflectivity) selection. To maximise the probability of cascade production, both

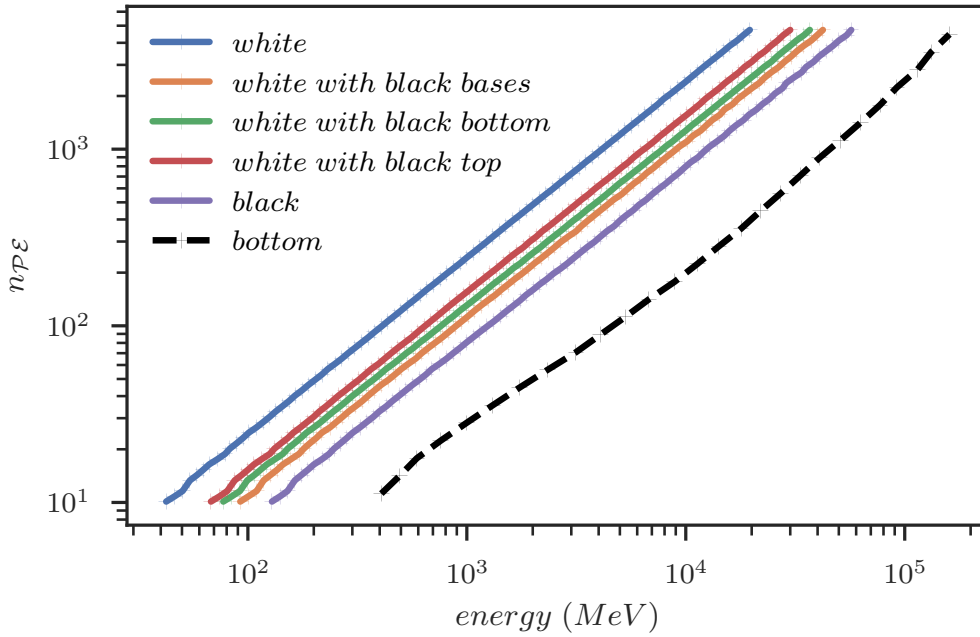


Figure 4: The number of p.e.s at different electromagnetic energy for upper chambers with different materials. The dashed black line shows the corresponding value for the lower chamber.

53 LHAASO and HAWC have a water depth $> 10 \times x_0$, where x_0 is the radiation length of high energy
 54 γ 's in water (~ 46 cm). However, both design also uses a material with low reflectivity (black) like
 55 Polypropylene. The upper chamber of the proposed DLWCD is shallow and narrower than these
 56 designs. The chamber also comprises reflective walls, namely, Tyvek used by the Pierre Auger
 57 Observatory [15] with a combination of black bases.

58 To compare the detection efficiency of the DLWCD, vertical γ 's were injected across the top
 59 of several design choices varying in aspect-ratio and material reflectivity (see Fig. 3). The DLWCD
 60 design, with white walls and a black top, has improved particle detection efficiency over both HAWC
 61 and LHAASO - like designs. A deeper chamber would ensure cascade production and subsequent
 62 detection of Cherenkov photons at ~ 100 MeV γ s, while a narrower chamber with reflective walls
 63 improves sensitivity to lower energy γ s. Reflective walls improve particle detection efficiency over
 64 non-reflective walls.

65 Additionally, high energy γ 's close to the shower core can result in the saturation of the upper
 66 PMT. To mitigate this, since these particles can also punch through into the lower chamber, the
 67 lower PMT can extend the dynamic range (see Fig. 4).

68 4. Angular Resolution

69 In order to compare the angular resolution of the DLWCD (upper - $\pi \times 1.91^2 \times 2.5$ m³) of
 70 different material combinations, we simulate vertical γ initiated showers at the centre of the array
 71 shown in Fig. 1. The angular resolution is then computed in several stages.

72 First, after requiring a minimum of 10 unit hits, a time difference of arrival of the shower hit
 73 first arrival times for each unit are used to compute the shower direction and time. Limiting the

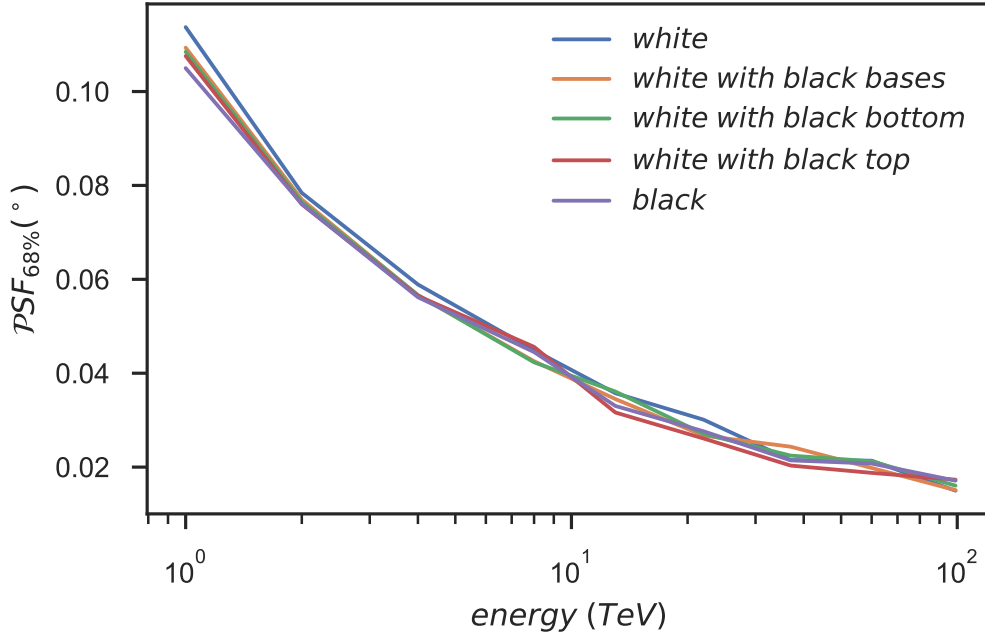


Figure 5: Angular resolution for 1 - 100 TeV vertical γ -ray's simulated with shower core at the center of an array of double-layered WCD's (upper - $\pi \times 1.91^2 \times 2.5 m^3$) with $\sim 80\%$ fill factor varying the material properties.

74 shower hits to 10% of the units hit with the largest charge limits the computational burden. A
 75 Landau fit to the arrival times as a function of distance to the shower core and charge is used to
 76 obtain mean and width parameters.

77 Given the Landau fit parameters, a 3-parameter likelihood fit (MINUIT [16]) is implemented
 78 to obtain the shower direction. The angular resolution is the 68 % containment of such showers
 79 (see Fig. 5).

80 We find that, as expected, as most of the first photons are the direct Cherenkov light, there is
 81 no or limited impact of the material combination on the angular resolution of the showers.

82 5. Gamma Hadron Separation

83 To evaluate the γ - hadron separation power, a Template-based maximum log-likelihood method
 84 comprising charge in the two chambers is implemented to discriminate between γ -ray and hadron
 85 induced air showers for an ensemble of γ -ray and proton-induced vertical showers of 1 to 100 TeV
 86 energy with the shower core located at the centre of the array. First, γ -ray and proton initiated
 87 showers are split into 70 – 30% training and test sets, respectively, with an exclusion region of
 88 40 m. The exclusion region is defined to account for the high transverse momentum of μ^\pm and
 89 punch-through of γ & e^\pm close to the shower core. The training set is then used to generate separate
 90 templates of charge in the upper and lower chambers for μ^\pm and e^\pm , & γ 's. The test set is then used
 91 to identify the likelihood of a μ^\pm on a tank-by-tank basis.

92 Once μ^\pm are tagged, the number of such particles is counted on an event-by-event basis for
 93 both γ and hadron initiated showers for a similar number of tanks hit. The γ and p^+ identification

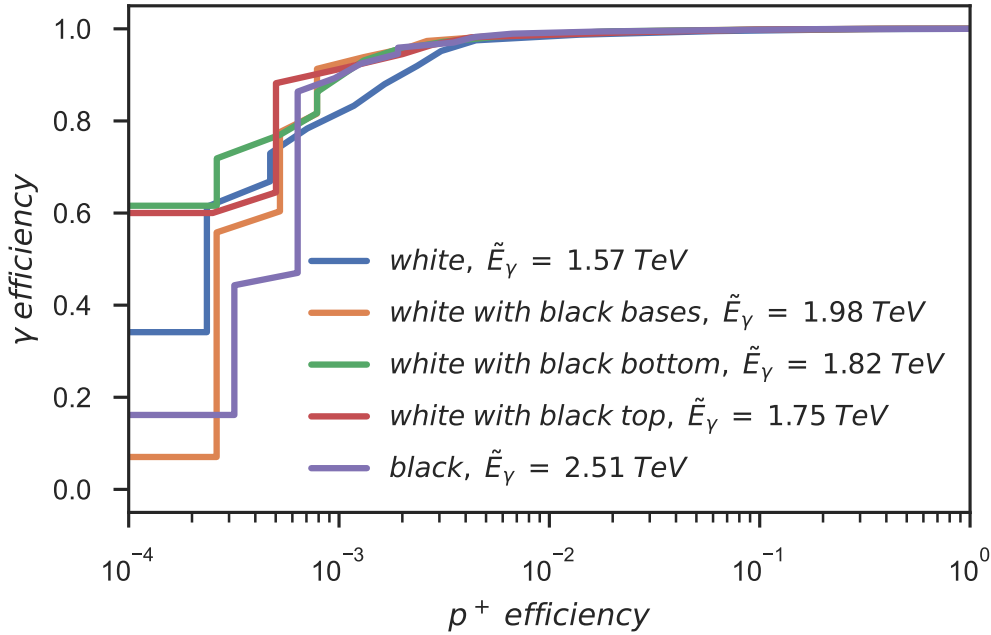


Figure 6: Gamma - Hadron separation efficiency for an array of double-layered WCD's (upper - $\pi \times 1.91^2 \times 2.5$ m³) with $\sim 80\%$ fill factor varying material reflectivity and an exclusion region of 40 m for $547 \leq nhits < 1280$.

94 efficiency is shown in Fig. 6 for different material combinations and $547 \leq nhits < 1280$. Tanks
 95 with a combination of white material represent showers with a lower median γ -ray energy. As
 96 expected while there is no significant difference in the γ - hadron separation power with different
 97 material combinations, with the combination of reflective material lower energy threshold can be
 98 achieved due to an increased particle detection efficiency.

99 6. Conclusion

100 The Southern Wide-field-of-view Gamma-ray Observatory (SWGO) will use the well-established
 101 and cost-effective technique of detecting Cherenkov light produced in water-filled detection units for
 102 TeV gamma-ray astronomy. Several detector technologies such as units with multiple photo-sensors
 103 and an option to deploy detector units in a lake are currently under investigation. The double-layered
 104 WCD leverages material and aspect ratio to enhance sensitivity, achieve excellent angular resolution
 105 and gamma hadron separation.

106 Acknowledgements

107 The SWGO Collaboration acknowledges the support from the agencies and organizations listed
 108 here: <https://www.swgo.org/SWGOwiki/doku.php?id=acknowledgements>.

109 **References**

- 110 [1] A. U. Abeysekara et al. (HAWC Collaboration), *Astrophys. J.* **843**, 39 (2017).
- 111 [2] G. D. Sciascio et al. (LHAASO Collaboration), *Nucl. Part. Phys. Proc.* **279 - 281**, 166-173
112 (2016).
- 113 [3] Z. Cao, F.A. Aharonian, Q. An et al. Ultrahigh-energy photons up to 1.4 petaelectronvolts
114 from 12 γ -ray Galactic sources. *Nature* 594, 33–36 (2021). [https://doi.org/10.1038/s41586-](https://doi.org/10.1038/s41586-021-03498-z)
115 [021-03498-z](https://doi.org/10.1038/s41586-021-03498-z)
- 116 [4] A. Albert et al. (SGSO Alliance), arXiv:1902.08429 (2019).
- 117 [5] J. Hinton (SWGGO Collaboration), *PoS ICRC2021* (2021) 023. [https://pos.sissa.it/](https://pos.sissa.it/395/023/pdf)
118 [395/023/pdf](https://pos.sissa.it/395/023/pdf)
- 119 [6] R. Conceicao (SWGGO Collaboration), *PoS ICRC2021* (2021) 707. [https://pos.sissa.](https://pos.sissa.it/395/707/pdf)
120 [it/395/707/pdf](https://pos.sissa.it/395/707/pdf)
- 121 [7] H. Goksu (SWGGO Collaboration), *PoS ICRC2021* (2021) 708. [https://pos.sissa.it/](https://pos.sissa.it/395/708/pdf)
122 [395/708/pdf](https://pos.sissa.it/395/708/pdf)
- 123 [8] H. Schoorlemmer et al., *Eur. Phys. J. C* **79**, 427 (2019). [https://doi.org/10.1140/epjc/](https://doi.org/10.1140/epjc/s10052-019-6942-x)
124 [s10052-019-6942-x](https://doi.org/10.1140/epjc/s10052-019-6942-x)
- 125 [9] S. Agostinelli et al., *Nucl. Instrum. Methods Phys. Res. A* **506** 205-303 (2003).
- 126 [10] Heck, D., et al., *CORSIKA: a Monte Carlo code to simulate extensive air showers*. (FZKA
127 6019)(Karlsruhe: Forschungszentrum Karlsruhe) (1998).
- 128 [11] S. Ostapchenko, *Phys. Rev. D* **83**, 014018 (2011). [https://doi.org/10.1103/PhysRevD.](https://doi.org/10.1103/PhysRevD.83.014018)
129 [83.014018](https://doi.org/10.1103/PhysRevD.83.014018)
- 130 [12] S.A.Bass et al. *Prog.Part.Nucl.Phys.* 41 (1998) 225
- 131 [13] M.Bleicher et al. *J.Phys.* G25 (1999) 1859
- 132 [14] Nelson, W. & Namito, Yoshihito. (1990). The EGS4 Code System: Solution of gamma-ray
133 and electron transport problems.
- 134 [15] I. Allekotte et al. (Pierre Auger Collaboration), *Nuclear Instruments and Methods in Physics*
135 *Research A* **586**, 409-420 (2008).
- 136 [16] F. James, MINUIT Function Minimization and Error Analysis: Reference Manual Version,
137 94.1, CERN-D-506 (2017)

138 **Full Authors List: SWGO Collaboration**

139 P. Abreu¹, A. Albert², E.O. Angüner³, C. Arcaro⁴, L.H. Arnaldi⁵, J.C. Arteaga-Velázquez⁶, P. Assis¹, A. Bakalová⁷, U. Bar-
 140 res de Almeida⁸, I. Batković⁴, J. Bellido⁹, E. Belmont-Moreno¹⁰, F. Bisconti¹¹, A. Blanco¹, M. Bohacova⁷, E. Bottacini⁴, T. Bretz¹²,
 141 C. Brisbois¹³, P. Brogueira¹, A.M. Brown¹⁴, T. Bulik¹⁵, K.S. Caballero Mora¹⁶, S.M. Campos¹⁷, A. Chiavassa¹¹, L. Chytka⁷,
 142 R. Conceição¹, G. Consolati¹⁸, J. Cotzomi Paleta¹⁹, S. Dasso²⁰, A. De Angelis⁴, C.R. De Bom⁸, E. de la Fuente²¹, V. de Souza²²,
 143 D. Depaoli¹¹, G. Di Sciascio²³, C.O. Dib²⁴, D. Dörner²⁵, M. Doro⁴, M. Du Vernois²⁶, T. Ergin²⁷, K.L. Fan¹³, N. Fraija⁸, S. Funk²⁸,
 144 J.I. García¹⁷, J.A. García-González²⁹, S.T. García Roca⁹, G. Giacinti³⁰, H. Goksu³⁰, B.S. González¹, F. Guarino³¹, A. Guillén³²,
 145 F. Haist³⁰, P.M. Hansen³³, J.P. Harding², J. Hinton³⁰, W. Hofmann³⁰, B. Hona³⁴, D. Hoyos¹⁷, P. Huentemeyer³⁵, F. Hueyotl-
 146 Zahuantitla¹⁶, A. Insolia³⁶, P. Janecek⁷, V. Joshi²⁸, B. Khelifi³⁷, S. Kunwar³⁰, G. La Mura¹, J. Lapington³⁸, M.R. Laspiur¹⁷,
 147 F. Leit²⁸, F. Longo³⁹, L. Lopes¹, R. Lopez-Coto⁴, D. Mandat⁷, A.G. Mariazzi³³, M. Mariotti⁴, A. Marques Moraes⁸, J. Martínez-
 148 Castro⁴⁰, H. Martínez-Huerta⁴¹, S. May⁴², D.G. Melo⁴³, L.F. Mendes¹, L.M. Mendes¹, T. Mineeva²⁴, A. Mitchell⁴⁴, S. Mohan³⁵,
 149 O.G. Morales Olivares¹⁶, E. Moreno-Barbosa¹⁹, L. Nellen⁴⁵, V. Novotny⁷, L. Olivera-Nieto³⁰, E. Orlando³⁹, M. Pech⁷, A. Pichel²⁰,
 150 M. Pimenta¹, M. Portes de Albuquerque⁸, E. Prandini⁴, M.S. Rado Cuchills⁹, A. Reisenegger⁴⁶, B. Reville³⁰, C.D. Rho⁴⁷, A.C. Rovero²⁰,
 151 E. Ruiz-Velasco³⁰, G.A. Salazar¹⁷, A. Sandoval¹⁰, M. Santander⁴², H. Schoorlemmer³⁰, F. Schüssler⁴⁸, V.H. Serrano¹⁷, R.C. Shellard⁸,
 152 A. Sinha⁴⁹, A.J. Smith¹³, P. Surajbali³⁰, B. Tomé¹, I. Torres Aguilar⁵⁰, C. van Eldik²⁸, I.D. Vergara-Quispé³³, A. Viana²², J. Vícha⁷,
 153 C.F. Vigorito¹¹, X. Wang³⁵, F. Werner³⁰, R. White³⁰, M.A. Zamalloa Jara⁹

154 ¹ Laboratório de Instrumentação e Física Experimental de Partículas (LIP), Av. Prof. Gama Pinto 2, 1649-003 Lisboa, Portugal
 155 ² Physics Division, Los Alamos National Laboratory, P.O. Box 1663, Los Alamos, NM 87545, United States
 156 ³ Aix Marseille Univ, CNRS/IN2P3, CPPM, 163 avenue de Luminy - Case 902, 13288 Marseille cedex 09, France
 157 ⁴ University of Padova, Department of Physics and Astronomy & INFN Padova, Via Marzolo 8 - 35131 Padova, Italy
 158 ⁵ Centro Atómico Bariloche, Comisión Nacional de Energía Atómica, S. C. de Bariloche (8400), RN, Argentina
 159 ⁶ Universidad Michoacana de San Nicolás de Hidalgo, Calle de Santiago Tapia 403, Centro, 58000 Morelia, Mich., México
 160 ⁷ FZU, Institute of Physics of the Czech Academy of Sciences, Na Slovance 1999/2, 182 00 Praha 8, Czech Republic
 161 ⁸ Centro Brasileiro de Pesquisas Físicas, R. Dr. Xavier Sigaud, 150 - Rio de Janeiro - RJ, 22290-180, Brazil
 162 ⁹ Academic Department of Physics – Faculty of Sciences – Universidad Nacional de San Antonio Abad del Cusco (UNSAAC), Av. de
 163 la Cultura, 733, Pabellón C-358, Cusco, Peru
 164 ¹⁰ Instituto de Física, Universidad Nacional Autónoma de México, Sendero Bicipuma, C.U., Coyoacán, 04510 Ciudad de México,
 165 CDMX, México
 166 ¹¹ Dipartimento di Fisica, Università degli Studi di Torino, Via Pietro Giuria 1, 10125, Torino, Italy
 167 ¹² RWTH Aachen University, Physics Institute 3, Otto-Blumenthal-Straße, 52074 Aachen, Germany
 168 ¹³ University of Maryland, College Park, MD 20742, United States
 169 ¹⁴ Durham University, Stockton Road, Durham, DH1 3LE, United Kingdom
 170 ¹⁵ Astronomical Observatory, University of Warsaw, Aleje Ujazdowskie 4, 00478 Warsaw, Poland
 171 ¹⁶ Facultad de Ciencias en Física y Matemáticas UNACH, Boulevard Belisario Domínguez, Km. 1081, Sin Número, Terán, Tuxtla
 172 Gutiérrez, Chiapas, México
 173 ¹⁷ Facultad de Ciencias Exactas, Universidad Nacional de Salta, Avda. Bolivia N° 5150, (4400) Salta Capital, Argentina
 174 ¹⁸ Department of Aerospace Science and Technology, Politecnico di Milano, Via Privata Giuseppe La Masa, 34, 20156 Milano MI,
 175 Italy
 176 ¹⁹ Facultad de Ciencias Físico Matemáticas, Benemérita Universidad Autónoma de Puebla, C.P. 72592, México
 177 ²⁰ Instituto de Astronomía y Física del Espacio (IAFE, CONICET-UBA), Casilla de Correo 67 - Suc. 28 (C1428ZAA), Ciudad
 178 Autónoma de Buenos Aires, Argentina
 179 ²¹ Universidad de Guadalajara, Blvd. Gral. Marcelino García Barragán 1421, Olímpica, 44430 Guadalajara, Jal., México
 180 ²² Instituto de Física de São Carlos, Universidade de São Paulo, Avenida Trabalhador São-carlense, nº 400, Parque Arnold Schimidt -
 181 CEP 13566-590, São Carlos - São Paulo - Brasil
 182 ²³ INFN - Roma Tor Vergata and INAF-IAPS, Via del Fosso del Cavaliere, 100, 00133 Roma RM, Italy
 183 ²⁴ Dept. of Physics and CCTVal, Universidad Tecnica Federico Santa Maria, Avenida España 1680, Valparaíso, Chile
 184 ²⁵ Universität Würzburg, Institut für Theoretische Physik und Astrophysik, Emil-Fischer-Str. 31, 97074 Würzburg, Germany
 185 ²⁶ Department of Physics, and the Wisconsin IceCube Particle Astrophysics Center (WIPAC), University of Wisconsin, 222 West
 186 Washington Ave., Suite 500, Madison, WI 53703, United States
 187 ²⁷ TUBITAK Space Technologies Research Institute, ODTU Campus, 06800, Ankara, Turkey
 188 ²⁸ Friedrich-Alexander-Universität Erlangen-Nürnberg, Erlangen Centre for Astroparticle Physics, Erwin-Rommel-Str. 1, D 91058
 189 Erlangen, Germany
 190 ²⁹ Tecnológico de Monterrey, Escuela de Ingeniería y Ciencias, Ave. Eugenio Garza Sada 2501, Monterrey, N.L., 64849, México
 191 ³⁰ Max-Planck-Institut für Kernphysik, P.O. Box 103980, D 69029 Heidelberg, Germany
 192 ³¹ Università di Napoli “Federico II”, Dipartimento di Fisica “Ettore Pancini”, and INFN Napoli, Complesso Universitario di Monte
 193 Sant’Angelo - Via Cinthia, 21 - 80126 - Napoli, Italy
 194 ³² University of Granada, Campus Universitario de Cartuja, Calle Prof. Vicente Callao, 3, 18011 Granada, Spain

- 195 ³³ IFLP, Universidad Nacional de La Plata and CONICET, Diagonal 113, Casco Urbano, B1900 La Plata, Provincia de Buenos Aires,
196 Argentina
- 197 ³⁴ University of Utah, 201 Presidents' Cir, Salt Lake City, UT 84112, United States
- 198 ³⁵ Michigan Technological University, 1400 Townsend Drive, Houghton, MI 49931, United States
- 199 ³⁶ Dipartimento di Fisica e Astronomia "E. Majorana", Catania University and INFN, Catania, Italy
- 200 ³⁷ APC-IN2P3/CNRS, Université de Paris, Bâtiment Condorcet, 10 rue A.Domon et Léonie Duquet, 75205 PARIS CEDEX 13, France
- 201 ³⁸ University of Leicester, University Road, Leicester LE1 7RH, United Kingdom
- 202 ³⁹ Department of Physics, University of Trieste and INFN Trieste, via Valerio 2, I-34127, Trieste, Italy
- 203 ⁴⁰ Centro de Investigación en Computación, Instituto Politécnico Nacional, Av. Juan de Dios Bátiz S/N, Nueva Industrial Vallejo,
204 Gustavo A. Madero, 07738 Ciudad de México, CDMX, México
- 205 ⁴¹ Department of Physics and Mathematics, Universidad de Monterrey, Av. Morones Prieto 4500, San Pedro Garza García 66238, N.L.,
206 México
- 207 ⁴² Department of Physics and Astronomy, University of Alabama, Gallalee Hall, Tuscaloosa, AL 35401, United States
- 208 ⁴³ Instituto de Tecnologías en Detección y Astropartículas (CNEA-CONICET-UNSAM), Av. Gral Paz 1499 - San Martín - Pcia. de
209 Buenos Aires, Argentina
- 210 ⁴⁴ Department of Physics, ETH Zurich, CH-8093 Zurich, Switzerland
- 211 ⁴⁵ Instituto de Ciencias Nucleares, Universidad Nacional Autónoma de México (ICN-UNAM), Cto. Exterior S/N, C.U., Coyoacán,
212 04510 Ciudad de México, CDMX, México
- 213 ⁴⁶ Departamento de Física, Facultad de Ciencias Básicas, Universidad Metropolitana de Ciencias de la Educación, Av. José Pedro
214 Alessandri 774, Ñuñoa, Santiago, Chile
- 215 ⁴⁷ Department of Physics, University of Seoul, 163 Seoulsiripdaero, Dongdaemun-gu, Seoul 02504, Republic of Korea
- 216 ⁴⁸ Institut de recherche sur les lois fondamentales de l'Univers (IRFU), CEA, Université Paris-Saclay, F-91191 Gif-sur-Yvette, France
- 217 ⁴⁹ Laboratoire Univers et Particules de Montpellier, CNRS, Université de Montpellier, F-34090 Montpellier, France
- 218 ⁵⁰ Instituto Nacional de Astrofísica, Óptica y Electrónica (INAOE), Luis Enrique Erro 1, Puebla, México
- 219